Journal of Materials Chemistry C

COMMUNICATION

Efficient NIR light blockage with matrix embedded silver nanoprism thin films for energy saving window coating†

Received 00th January 20xx,
Accepted 00th January 20xx

DOI: 10.1039/x0xx00000x

www.rsc.org/

M. Carboni,[a,b,c] M. Carravetta,[a] XL. Zhang,[c]* E. Stulz[a]*

Highly efficient composite films, consisting of silica coated and functionalised silver nanoprisms (SNPs) are presented as low–cost material to reduce thermal radiation flux with reduced impact on daylight transmission compared to similar solutions. The SNPs are covalently embedded in a poly(methyl methacrylate) (PMMA) matrix which prevents both leaking of the NPs and aggregation within the matrix, thus enabling the formation of stable thin films with controllable dispersion. The cast thin films show absorbance in the IR region above 700 nm and a figure of merit around 1 which is achieved with very thin films and low material consumption.

Introduction

Windows are regarded as one of the weakest elements in buildings with regards to insulation, leading to a rather high energy consumption due to either heating or cooling of the interior space. Although improvements have been achieved in reducing the heat transfer through convection and conductions, reducing heat transfer without hampering the light income is still challenging. In this communication we report a composite film made of silica coated and functionalised triangular silver nanoprisms (SNPs) which are covalently embedded in a poly(methyl methacrylate) (PMMA) matrix as low-cost material to reduce thermal radiation flux with lowered impact on daylight transmission.

The energy demand from residential buildings will show an average growth of approximately 0.6% every year until 2040 according to the latest Annual Energy Outlook.[1] Projections show that this increase will be due to cooling rather than heating as a result of the higher portion of urbanisation in warmer climate zones. The interest in technologies that can reduce the consumption of energy for heating or cooling buildings and vehicles therefore is steadily growing. In particular, the glazing of buildings offers great potential for energy saving as these account for about 30% of total energy loss due to their high *U-value* (~0.8 W/m^2K) compared to other elements of the building envelope. Currently, the research is focusing on reducing the heat exchange, which is induced by radiative transfer, through direct coating of the glass. So far reflective coatings made of metal or metal oxide films are the materials of choice in commercial applications, but concern emerges regarding their extensive use in urban area, particularly the formation of heating islands due to the reflection of the infrared radiation.[2] The use of absorbing materials, on the other hand, is still limited due to the high impact on the visible light income through the windows. Although "smart" devices which are able to switch from a bleached (colourless) to a coloured state are known (such as electrochromic or termochromic materials),[3-6] some issues still limit their use, which include durability, high material cost, switching time and deposition method.[7, 8]

The use of metal nanoparticles (MNPs) as dyes for energy saving coatings is gaining interest as these materials show a strong extinction (absorption and scattering) due to the surface plasmon resonance (SPR), and no photo-bleaching. Although MNPs usually show extinction in the visible part of the light, their unique characteristics allows to precisely control the resonance wavelength. Particles size, shape and surrounding media are among the factors affecting the spectral position and number of the peaks.[9, 10] By modifying one or more of these parameters, the extinction maximum can be shifted to lower energy, and eventually near infrared radiation can be absorbed without affecting the visible light transmission. In principle, due to the high extinction coefficient of MNPs, high absorbance can be achieved through low concentration of particles, which effectively reduces the cost for solar control coating. *Xu et al.*[11] have calculated that the cost of coatings made using gold nanorods dispersed in a poly(vinyl alcohol) (PVA) matrix (0.26 g Au/m^2) would be of ~3.76 USD/m^2 compared to the average price of ~100 USD/m^2 of currently available technologies.

[a.] School of Chemistry & Institute for Life Sciences, University of Southampton, Highfield, Southampton SO17 1BJ, UK; *E-mail: est@soton.ac.uk
[b.] current address: Building Energy Materials and Components, EMPA, 8600 Dübendorf, Switzerland.
[c.] Engineering and the Environment, University of Southampton, Highfield, Southampton SO17 1BJ, UK; *E-mail: XL.Zhang@soton.ac.uk

† Electronic Supplementary Information (ESI) available: synthetic procedures and full characterisation of the composites. See DOI: 10.1039/x0xx00000x

Pioneering work by *Schelm et al*.[12, 13] using LaB_6 nanoparticles, which were dispersed in a poly(vinylbutyral) (PVB) matrix and sandwiched between two glass slides, demonstrated the feasibility of this approach. Reporting good figures of merit (FOM) in terms of the ratio between the visible and the solar transmitted light (T_{lum} and T_{sol}), the LaB_6 particles outperform ITO based systems. NIR absorbing gold nanorods dispersed in a PVA matrix have recently been employed for window coatings by *Stokes et al*.[14] These coatings absorb the NIR radiation up to 60 % and show a good T_{lum} of around 40 %.

Although these coatings are very promising, they still show some extinction in the visible spectrum which could hinder their use in many applications such as glazing. Furthermore, simply dispersing the particles into a polymeric matrix could lead to aggregation of the particles, i.e. change in their optical properties, and their leaching into the environment. Here we present the use of triangular silver nanoprisms (SNPs) as suitable material for MNP based energy saving coating.[15-20] We have chosen polymethyl-methacrylate (PMMA) as polymeric host as it does not show yellowing upon ageing, and due to its robustness under outdoor conditions; PMMA shows improved properties when doped with either silica[21] or silver nanoparticles.[22] The nano-composites were prepared with different degree of polymerisation of PMMA and different SNP loading, and characterised using NMR and IR spectroscopy, GPC, TGA and TEM. The composites were deposited onto glass slides, and their efficiency in selectively absorbing the NIR portion[22] of the spectrum without affecting the transmittance of the visible radiation was evaluated. To avoid aggregation of the metal nuclei in the polymeric host, SNPs were coated with a silica shell (SNP@SiO_2) acting as an optically transparent protecting layer (**Scheme 1**). To create a stable dispersion of the SNP@SiO_2 in PMMA, the particles were further functionalised with allyl groups and polymerised with methylmethacrylate to form covalent SNP@SiO_2/PMMA composites, which is a major step towards the formation of stable, non-leaching inclusion coatings. The solution was drop-casted onto glass slides and the optical properties of the films were determined as the ratio of T_{lum} / T_{sol}. To our knowledge we report the first covalently embedded polymer-NP composite with favourable optical properties suitable for windows coating; related systems include the formation of composites consisting of Al, Ag, Au, Cu, Pt, ZnO and Fe nanoparticles embedded in polyacrylate, Teflon, polyvinyl(methyl ketone), poly(vinyl pyrrolidone), polyenthylene, polydimethylsiloxane or PMMA.[21, 23-29]

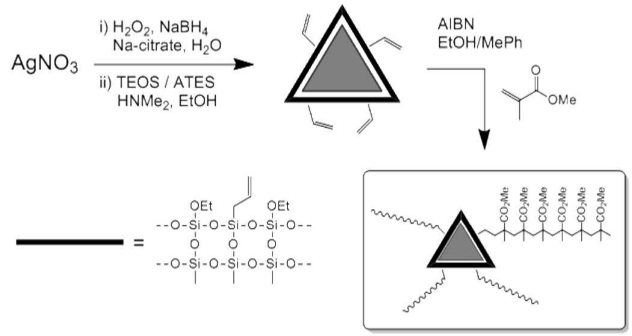

Scheme 1. Synthesis SNP@SiO_2/PMMA composite. TEOS = tetraethoxy silane, ATES = allyl triethoxy silane.

Results and Discussion

The synthesis of the SNPs was conducted in bulk by adapting previously published methods[20, 30, 31] and as described in the experimental section in the supporting information (ESI). In this way, SNPs with an average size of 39±8 nm were obtained (**SNP-1**), according to TEM measurements (**Figure 1**). Previous studies reported that chloride ions generally led to a size increase of silver nanoprisms.[32] Addition of KCl prior to the reducing agent shows this effect also here, and the sizes of the SNPs increases to an average of 59±16 nm (**SNP-2**). This also has an impact on the optical properties of the SNPs (**Figure 1**). While the smaller size SNP-1 show an extinction maximum around 620 nm, the larger size SNP-2 show a shift of the extinction to lower energy at around 750 nm with a concomitant lower extinction in the higher energy part of the visible spectrum, which is beneficiary for the anticipated application. The peak for SNP-2 also is broader due to sharper tips of the prisms, which was reported by *Sherry et al* as a lightning rod effect.[17] It is worth noting that the extinction spectra of the MNPs are a result of a combination of absorption and scattering.[26] It is well understood that the contribution of the scattering increases with the size of the MNPs, with shape and surrounding environment also contributing. The contribution of the scattering to the extinction was calculated for triangular silver disks, where it was found that it is negligible for MNPs <25 nm, while it becomes an important factor for MNPs above 50 nm, and is predominant for large MNPs of >100 nm size. Scattering is in our case clearly not negligible, but absorption still remains the dominant contribution to the overall extinction.

The coating of nanoparticles with silica shells has been established with various metallic nanoparticles including silver, and has proven to be advantageous for MNP coating due to its stability, transparency and availability for further functionalization through sol-gel chemistry.[33-37] Adopting *Mirkin's* approach,[35] the SNPs were first stabilized by surface functionalization with mercapto-hexanoic acid, followed by growth of the silica shell in a TEOS solution using dimethylamine (DMA) as catalyst to give SNP@SiO_2. As reported previously,[26] the coating with silica leads to a further red-shift by ~70 nm, which can be related to a shell thickness of approximately 15 nm. The successful formation of the silica shell can be seen in the TEM images of both (SNP-1)@SiO_2 and (SNP-2)@SiO_2 (**Figure 1**). To add functionality, SNP@SiO_2 were formed in the presence of allyl-triethoxysilane (ATES). Co-condensation of TEOS with ATES was preferred over post−functionalization of the silica surface which gave functionalization with better reproducibility. Using different TEOS / ATES ratios, the resulting silica shell becomes thinner due to shell growth blockage by ATES, leading to smaller red-shifts of the absorbance (see Figure S1 in ESI for details). Energy-dispersive X-ray spectroscopy (EDAX) also shows strong reduction of Si counts compared to Ag counts upon addition of higher amounts of ATES (Figure S1). The IR spectrum of allyl-SNPs mainly shows signals due to the silicate shell, but weak peaks at 2919 cm^{-1} and 2850 cm^{-1}, and at 1430 cm^{-1} are characteristic of the attached allyl-silane moiety (Figure S2).[38]

The addition of allyl-groups to the SNP@SiO_2 is crucial for the formation of stable polymer inclusion systems through covalent attachment of the SNPs to the polymer matrix; this also improves the dispersion of the SNPs within the matrix. To produce the SNP@SiO_2/PMMA composites, the polymer was grown in the presence of various amounts of SNP@SiO_2 (see ESI for details). After polymerisation, the PMMA was precipitated in cold methanol, collected on a filter and washed thoroughly with methanol. No SNPs were detected in the filtrate, showing the stable inclusion within the polymer matrix through grafting without leakage of the SNPs, which is a prerequisite to form useful long-lived window coatings. The IR spectrum of PMMA is not affected by the presence of the SNPs (Figure S2). To evaluate the effect of SNPs on the chain length of the polymer, PMMA was prepared with different AIBN concentration (1 %, 2 %, 4 % and 6%) in the presence of different amounts of allyl-SNP (0, 0.1 %, 0.2 % and 0.5 % w/w; Table S1 in ESI), and the average M_n and M_w of PMMA was determined using size exclusion chromatography (SEC). No clear trends can be observed upon addition of different amounts of allyl-SNPs, and only at 0.1 % loading somewhat higher M_n and M_w values compared to polymerization in absence of allyl-SNPs were seen. Since the lowest AIBN concentration (1 %) gave the longest polymer chains, further experiments were conducted using these conditions.

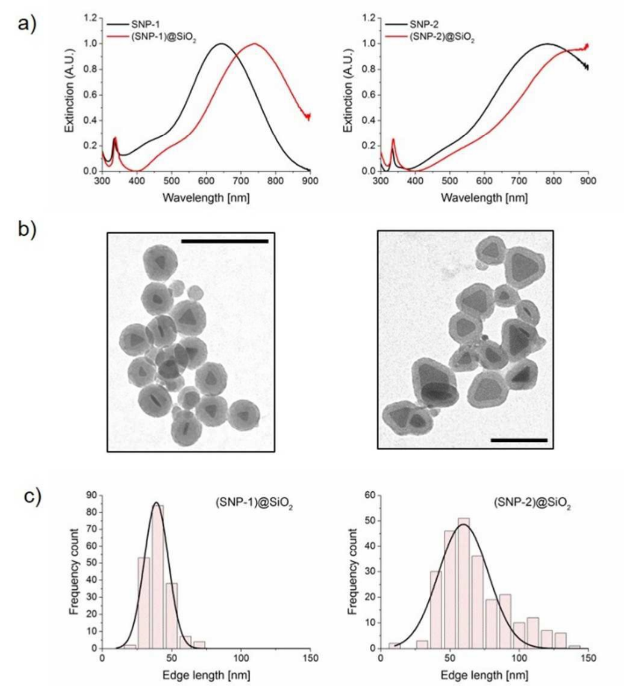

Figure 1. Characterisation of the SNPs, showing (SNP-1)@SiO_2 in the left panel (prepared in the absence of chloride), and (SNP-2)@SiO_2 in the right panel (prepared in the presence of chloride). a) Extinction spectra of SNPs, before (black line) and after (red line) coating with TEOS; b) TEM pictures of SNP@SiO_2, scale bar = 200 nm; c) size distribution of SNP@SiO_2 obtained from the TEM measurements with *Gaussian* fitting curve for average size determination.

The SNP@SiO_2/PMMA composites show a three-stage thermal degradation as determined by TGA, which is shown in **Figure 2** for SNP-1. The first two stages at ~165 °C and ~270 °C, which have been assigned to the scission of the head-to-head linkages and to radical induced degradation,[39, 40] are largely unaffected by the presence of the SNPs. The third degradation event at ~360 °C, which is associated with random scission, shows a reduction of about 10 °C with increasing amount of the allyl-SNP@SiO_2. This is in contrast to what has been reported for bare spherical AuNPs[22] and PdNPs[41] which stabilise the PMMA matrix. Nevertheless, the loss in thermal stability is minimal at the expected working conditions. The covalent attachment of PMMA to the allyl-SNPs was also confirmed by NMR spectroscopy (**Figure 2**). A sample of 6.5 g of (SNP-1)@SiO_2/PMMA composite (0.5 % SNP) was repeatedly washed with chloroform until no more unbound polymer was extracted, which required six washings. The majority of unbound polymer (99.4 %) was removed during the first washing (Figure S3 and Table S2). Using magic-angle spinning (MAS) solid state NMR spectroscopy and ramped cross-polarization (CP),[42] the ^{13}C signals of PMMA can clearly be recognised in the SNP@SiO_2/PMMA composites. The small shifts of the signals of PMMA in the bound state are compatible with a covalent connection between the SNPs and PMMA.

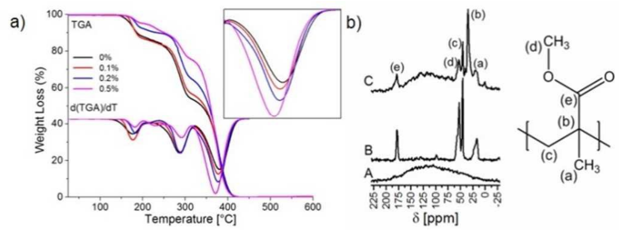

Figure 2. a) TGA and first derivative measured for (SNP-1)@SiO_2/PMMA composite prepared with different SNP percentage (0 %, 0.1 %, 0.2 % and 0.5 % w/w) using 1 % AIBN, the inset shows and expansion of the third stage; b) CP MAS ^{13}C solid-state NMR spectrum of (SNP-1)@SiO_2/PMMA after removal of the physisorbed polymer by centrifugation and washing; A: (SNP-1)@SiO_2, B: PMMA reference sample, C: (SNP-1)@SiO_2/PMMA.

Thin films of both (SNP-1)@SiO_2/PMMA and (SNP-2)@SiO_2/PMMA) were prepared by slow evaporation of a chloroform suspension of the composites. Use of toluene or other solvents led to rather thick (>1 mm) and fragile films. The optimal concentration was found to be 20 % of composite and produced films of 0.1 mm thickness with good visible transparency. The transmission spectra show strong absorbance at shorter wavelengths (<1000 nm) due to the SNPs (**Figure 3**), where the peak for the SNP-2 system is broader and has a maximum at a higher wavelength of 880 nm compared to the SNP-1 system (740 nm); this is analogous the absorbance of the SNPs on their own.

To evaluate the efficiency of the composites as energy saving materials, the ratio between the transmittance of visible light (T_{lum}) and the transmittance of total solar radiation (T_{sol}) was taken into account as FOM. The ideal value of the FOM would be 2.08, corresponding to a material absorbing all the NIR radiation while passing all UV and visible light, but usually values above 1 are aimed at.[14] The FOM values (**Table 1**, Figure S4) are higher for the (SNP-2)@SiO_2/PMMA than for the (SNP-1)@SiO_2/PMMA composites, with higher loading of SNP leading to a reduction of the FOM due to higher absorbance in the visible region. The best value was obtained for the system (SNP-2)@SiO_2/PMMA at 0.1 % SNP loading (FOM 1.011), showing that this system has characteristics very suitable for efficiently blocking the low energy light while not greatly disturbing the visual impact. This is particularly the case as the films are thin and contain a low loading of silver nanoprisms.

Table 1. FOM for NP composites with variable NP loading and film thickness.

Composite	NP loading	Film thickness [mm]	T_{lum}	T_{sol}	FOM [a)]
(SNP-1)@SiO_2/PMMA	0.1 %	0.1	0.927	0.929	0.997
		0.8	0.410	0.416	0.985
	0.2 %	0.1	0.816	0.830	0.982
		0.8	0.541	0.567	0.953
	0.5 %	0.1	0.575	0.619	0.928
(SNP-2)@SiO_2/PMMA	0.1 %	0.1	0.909	0.899	1.011
		0.8	0.517	0.487	1.063
	0.2 %	0.1	0.895	0.893	1.003
		0.8	0.463	0.453	1.022
	0.5 %	0.1	0.586	0.601	0.975
AuNR/PVA [a)]	Pane 1	0.8	0.37	0.37	1.000
	Pane 2	0.8	0.30	0.29	1.030
LaB_6/PVB [b)]	0.02 %	0.8	0.624	0.366	1.705
	0.025 %	0.8	0.575	0.314	1.705
	0.03 %	0.8	0.530	0.274	1.934

[a)] Data taken from ref. [13], NP loading not given; [b)] Data taken from ref. [11].

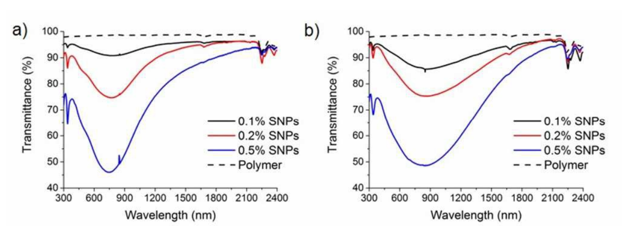

Figure 3. UV-vis-NIR transmittance of thin films of SNP@SiO_2/PMMA prepared with SNP-1 (a) and SNP-2 (b), at 0.1 %, 0.2 % and 0.5 % of SNP filler amount, including pure polymer for comparison.

The FOM measured here is comparable to the FOM reported for gold nanorods (AuNR) in PVA (1.000 – 1.030) where AuNRs were mixed into 15 wt% PVA solutions in various ratios,[14] but is lower than for films prepared with LaB_6 nanoparticles (FOM 1.705 – 1.934, 0.02 % – 0.03 % NP loading).[12] However, two considerations should be taken into account: firstly the reported films are 0.8 mm thick, and secondly different polymer matrices were used. Creating 0.8 mm films shows an improved FOM for (SNP-2)@SiO_2/PMMA, which is maximal at 0.1 % SNP loading (1.063). At 0.2 % SNP-2 loading some improvement in the FOM can also be seen, whereas for 0.5 % SNP loading the films become visibly black with little light trasmittance for both SNP-1 and SNP-2. In comparison, the correspondingly high FOM for LaB_6 is also influenced by the inherently high near-IR absorbance of the PVB matrix used. PVB has a transmittance of ~70 % in the visible light whereas PMMA is 100 % transmitting, and the FOM of pure PVB was calculated to be ~1.2 which in itself is higher than the NP systems. In this respect, the use of thin PMMA films with low SNP loading shows great advantage over other films.

Conclusions

In summary, we have demonstrated efficient NIR light blockage of silver nanoprisms that are covalently incorporated into PMMA matrices to form thin film glass coating, whilst still being largely transmitting in the visible light region. The covalent embedding in the polymer matrix is a great advantage as it prevents both leaking of the NPs and aggregation within the matrix, thus enabling the formation of stable thin films with controllable dispersion. The polymerisation and the properties of the matrix are not significantly affected by the presence of the SNPs. Batch synthesis of SNPs in the presence of chloride, followed by simultaneous silica coating and functionalization produces the most suitable particles. The cast thin films show absorbance in the IR region above 700 nm and FOM which are comparable to other systems albeit achieved with much thinner films and lower material consumption. Even though some blockage of the visible light cannot yet be completely avoided, the system has a much lower impact to the perception of the light blockage. This should lay the foundation to further explore this system for the creation of suitable window coatings which show reduced heat loss in buildings and vehicles, or indeed any other application where IR blockage is desired.

Acknowledgements

Financial support by ERDF (ISCE:Chem & InterReg IVa program 4061) and an EPSRC DTC for Carboni is greatly acknowledged. Carravetta acknowledges the Royal Society for a University Research Fellowship.

Notes and references

1 Annual Energy Outlook 2015, U.S. Energy Information Administration, Washington, DC 20585, US, 2015
2 N. J. Shih and Y. S. Huang, *Build. Res. Informat.*, 2001, **29**, 30-39.
3 S. Y. Li, G. A. Niklasson and C. G. Granqvist, *J. Appl. Phys.*, 2014, **115**.
4 C. G. Granqvist, P. C. Lansaker, N. R. Mlyuka, G. A. Niklasson and E. Avendano, *Sol. Energy Mater. Sol. Cells*, 2009, **93**, 2032-2039.
5 E. Avendano, A. Azens, G. A. Niklasson and C. G. Granqvist, *Sol. Energy Mater. Sol. Cells*, 2004, **84**, 337-350.
6 C. G. Granqvist, *Sol. Energy Mater. Sol. Cells*, 2000, **60**, 201-262.
7 C. M. Lampert, *Sol. Energy Mater. Sol. Cells*, 2003, **76**, 489-499.
8 N. A. O'Brien, J. Gordon, H. Mathew and B. P. Hichwa, *Thin Solid Films*, 1999, **345**, 312-318.
9 K. L. Kelly, E. Coronado, L. L. Zhao and G. C. Schatz, *J. Phys. Chem. B*, 2003, **107**, 668-677.
10 W. Caseri, *Macromol. Rapid Commun.*, 2000, **21**, 705-722.
11 X. Xu, T. H. Gibbons and M. B. Cortie, *Gold Bull.*, 2006, **39**, 156-165.
12 S. Schelm, G. B. Smith, P. D. Garrett and W. K. Fisher, *J. Appl. Phys.*, 2005, **97**.
13 S. Schelm and G. B. Smith, *Appl. Phys. Lett.*, 2003, **82**, 4346-4348.
14 N. L. Stokes, J. A. Edgar, A. M. McDonagh and M. B. Cortie, *J. Nanopart. Res.*, 2010, **12**, 2821-2830.
15 D. Aherne, D. M. Ledwith, M. Gara and J. M. Kelly, *Adv. Funct. Mater.*, 2008, **18**, 2005-2016.
16 K. Munechika, J. M. Smith, Y. Chen and D. S. Ginger, *J. Phys. Chem. C*, 2007, **111**, 18906-18911.
17 L. J. Sherry, R. C. Jin, C. A. Mirkin, G. C. Schatz and R. P. Van Duyne, *Nano Lett.*, 2006, **6**, 2060-2065.
18 R. Zmijan, M. Carboni, L. Capretto, E. Stulz and X. L. Zhang, *RSC Adv.*, 2014, **4**, 14569-14572.
19 M. Carboni, L. Capretto, D. Carugo, E. Stulz and X. L. Zhang, *J. Mater. Chem. C*, 2013, **1**, 7540-7546.
20 G. S. Métraux and C. A. Mirkin, *Adv. Mater.*, 2005, **17**, 412-415.
21 J. de la Venta, A. Pucci, E. Fernández Pinel, M. A. García, C. de Julián Fernandez, P. Crespo, P. Mazzoldi, G.

Ruggeri and A. Hernando, *Adv. Mater.*, 2007, **19**, 875-877.

22 V. V. Vodnik, J. V. Vukovic and J. M. Nedeljkovic, *Colloid Polym. Sci.*, 2009, **287**, 847-851.

23 F. Bauer, H.-J. Gläsel, U. Decker, H. Ernst, A. Freyer, E. Hartmann, V. Sauerland and R. Mehnert, *Progress in Organic Coatings*, 2003, **47**, 147-153.

24 A. Biswas, H. Eilers, F. H. Jr, O. C. Aktas and C. V. S. Kiran, 2006, **88**, 013103.

25 N. Cioffi, N. Ditaranto, L. Torsi, R. A. Picca, E. D. Giglio, L. Sabbatini, L. Novello, G. Tantillo, T. Bleve-Zacheo and P. G. Zambonin, *Anal Bioanal Chem*, 2005, **382**, 1912-1918.

26 D. Crespy and K. Landfester, *Polymer*, 2009, **50**, 1616-1620.

27 A. Goyal, A. Kumar, P. K. Patra, S. Mahendra, S. Tabatabaei, P. J. J. Alvarez, G. John and P. M. Ajayan, *Macromol. Rapid Commun.*, 2009, **30**, 1116-1122.

28 S. Soumya, A. P. Mohamed, K. Mohan and S. Ananthakumar, *Sol. Energy Mater. Sol. Cells*, 2015, **143**, 335-346.

29 J. L. Wilson, P. Poddar, N. A. Frey, H. Srikanth, K. Mohomed, J. P. Harmon, S. Kotha and J. Wachsmuth, *J. Appl. Phys.*, 2004, **95**, 1439-1443.

30 R. C. Jin, Y. C. Cao, E. C. Hao, G. S. Métraux, G. C. Schatz and C. A. Mirkin, *Nature*, 2003, **425**, 487-490.

31

32 R. C. Jin, Y. W. Cao, C. A. Mirkin, K. L. Kelly, G. C. Schatz and J. G. Zheng, *Science*, 2001, **294**, 1901-1903.

33 N. Cathcart, A. J. Frank and V. Kitaev, *Chem. Commun.*, 2009, 7170-7172.

34 Y. Kobayashi, H. Katakami, E. Mine, D. Nagao, M. Konno and L. M. Liz-Marzan, *J. Colloid Interface Sci.*, 2005, **283**, 392-396.

35 L. M. Liz-Marzan, M. Giersig and P. Mulvaney, *Langmuir*, 1996, **12**, 4329-4335.

36 C. Xue, X. Chen, S. J. Hurst and C. A. Mirkin, *Adv. Mater.*, 2007, **19**, 4071-4074.

37 S. H. Liu and M. Y. Han, *Chem.-Asian J.*, 2010, **5**, 36-45.

38 K. W. Shah, T. Sreethawong, S. H. Liu, S. Y. Zhang, L. S. Tan and M. Y. Han, *Nanoscale*, 2014, **6**, 11273-11281.

39 Y. S. Chaudhary, J. Ghatak, U. M. Bhatta and D. Khushalani, *J. Mater. Chem.*, 2006, **16**, 3619-3623.

40 L. E. Manring, *Macromolecules*, 1991, **24**, 3304-3309.

41 T. Kashiwagi, A. Inaba, J. E. Brown, K. Hatada, T. Kitayama and E. Masuda, *Macromolecules*, 1986, **19**, 2160-2168.

42 C. Aymonier, D. Bortzmeyer, R. Thomann and R. Mullhaupt, *Chem. Mater.*, 2003, **15**, 4874-4878.

43 G. Metz, X. L. Wu and S. O. Smith, *J. Magn. Res. Series A*, 1994, **110**, 219-227.

Table of contents entry

Efficient NIR light blockage with matrix embedded silver nanoprism thin films for energy saving window coating

Highly efficient composite films, consisting of silica coated and functionalised silver nanoprisms (SNPs) which are covalently embedded in a PMMA matrix, are presented as low−cost material to reduce thermal radiation flux with low impact on daylight transmission. The covalent embedding in the polymer matrix is a great advantage as it prevents both leaking of the NPs and aggregation within the matrix, thus enabling the formation of stable thin films with controllable dispersion.